# SUPPORTING MATERIAL

### Theoretical analysis of a simple model network

We consider a simple model "network" (Fig. 5) consisting of elastic elements that form and break stochastically with constant average rates $k^+$ and $k^-$ such the steady-state number of elements $n_L = k^+/k^-$. The left side of the network is fixed with the right side subjected to a constant applied stress $\sigma$. The resulting deformation is resisted by an elastic stress $\sigma_e$ which is the sum of all elastic forces on individual elements and a viscous stress $\sigma_v = \zeta\dot{\varepsilon}$ where $\dot{\varepsilon}$ is the strain rate, and $\zeta$ is a drag coefficient which we assume to be a small constant. Assuming a constant average strain rate $\dot{\varepsilon}_{avg}$ at steady state (see below), the distribution of strains across individual network elements is given by:

$$P(\varepsilon) = \frac{\dot{\varepsilon}_{avg}}{k^-}\exp\left(-\frac{k^-}{\dot{\varepsilon}_{avg}}\varepsilon\right) \tag{S1}$$

We initially consider the case where the force-extension curve for individual elements is linear:

$$F_i = K\varepsilon_i \tag{S2}$$

where $\varepsilon_i$ is strain on the $i$th element and $K$ is its stiffness. The force balance on the network is given by:

$$\zeta\dot{\varepsilon} = \sigma - \sigma_e \tag{S3}$$

and the rate of change of $\sigma_e$ as the links form, strain, and break can be written:

$$\dot{\sigma}_e = n_L K\dot{\varepsilon} - k^-\sum_{n_L} F_i = n_L K\dot{\varepsilon} - k^-\sigma_e \tag{S4}$$

The first and second terms in Eq. S4 represent force buildup and dissipation due to stretching and breaking of existing elements, respectively, and $n_L K$ corresponds to the elastic modulus of the entire network, $E_0$. Setting $\dot{\sigma}_e = 0$ and solving Eqs. S3 and S4 simultaneously for $\sigma_e$ and constant $\dot{\varepsilon}$ yield the asymptotically stable state:

$$\dot{\varepsilon} = \frac{k^- \sigma}{k^- \zeta + n_L K}$$
$$\sigma_e = \frac{n_L K \sigma}{k^- \zeta + n_L K} \tag{S5}$$

Note that for $\zeta \ll n_L K / k^-$, this reduces to:

$$\dot{\varepsilon} \sim \frac{k^- \sigma}{n_L K}$$
$$\sigma_e \sim \sigma \tag{S6}$$

Thus, for the simple case of linear force-extension, $\dot{\varepsilon}$ is always proportional to the magnitude of $\sigma$, and the effective viscosity is the elastic modulus of the network divided by the turnover rate: $\eta_{\text{eff}} = \sigma / \dot{\varepsilon} \sim n_L K / k^- = E_0 / k^-$.

Now, consider the case in which the individual springs have a non-linear force-extension curve. For simplicity, we assume that:

$$F(\varepsilon) = \begin{cases} K\varepsilon & \text{if } \varepsilon < \varepsilon_c \\ \infty & \text{if } \varepsilon \geq \varepsilon_c \end{cases} \tag{S7}$$

When a single element exceeds $\varepsilon_c$, deformation is stalled until the element turns over. Then, assuming negligible viscous drag, the network will deform at the linear rate:

$$\dot{\varepsilon}_{\text{lin}} = \frac{k^- \sigma}{n_L K} \tag{S8}$$

until the next element crosses the strain threshold. In response to a constant $\sigma$, therefore, the average strain rate will be:

$$\dot{\varepsilon}_{\text{avg}} = \frac{\Delta\varepsilon_{\text{avg}}}{\Delta t_{\text{avg}} + \frac{1}{k^-}} \tag{S9}$$

where $\Delta\varepsilon_{\text{avg}}$ is the average strain increment required to bring the next element to threshold, $\Delta t_{\text{avg}}$ is the time required to achieve that increment at the rate $\dot{\varepsilon}_{\text{lin}}$, and $1 / k^-$ is the lifetime of the strained element. Using $\Delta t_{\text{avg}} = \Delta\varepsilon_{\text{avg}} / \dot{\varepsilon}_{\text{lin}}$, we have:

$$\dot{\varepsilon}_{\text{avg}} = \frac{\Delta\varepsilon_{\text{avg}}}{\frac{\Delta\varepsilon_{\text{avg}} n_{\text{L}} K}{k^{-}\sigma} + \frac{1}{k^{-}}} = \frac{k^{-}\sigma\Delta\varepsilon_{\text{avg}}}{\Delta\varepsilon_{\text{avg}} n_{\text{L}} K + \sigma} \tag{S10}$$

Regardless of details, $\Delta\varepsilon_{\text{avg}}$ will decrease monotonically with $\sigma$. Thus, for non-linear force-extension, the model predicts a crossover at $\sigma_{\text{th}} \sim \Delta\varepsilon_{\text{avg}} n_{\text{L}} K$ from a regime where $\dot{\varepsilon}$ is directly proportional to $\sigma$ ($\dot{\varepsilon}_{\text{avg}} \sim k^{-}\sigma / n_{\text{L}} K$) to one where $\dot{\varepsilon}$ is independent of $\sigma$ ($\dot{\varepsilon}_{\text{avg}} \sim k^{-}\Delta\varepsilon_{\text{avg}}$). For both regimes, the predicted strain rate is directly proportional to network turnover rate $k^{-}$, again as observed in simulations. Finally, note that when the viscous and elastic contributions to $\eta_{\text{eff}}$ are comparable, magnitudes at low $\sigma$ as observed in Fig. 1*E* ($\zeta \sim n_L K / k^{-}$), then Eq. S10 becomes:

$$\dot{\varepsilon}_{\text{avg}} = \frac{k^{-}\sigma\Delta\varepsilon_{\text{avg}}}{\Delta\varepsilon_{\text{avg}}\left(n_{\text{L}} K + k^{-}\zeta\right) + \sigma} \tag{S11}$$

The transition from stress-dependent (linear) to stress-independent (non-linear) creep regime still occurs, albeit at a slightly higher $\sigma_{\text{th}}$.

**Parallel computation**

We implemented the computational model in the C language and employed parallel computations using the Message Passing Interface (MPI) with spatial domain decomposition. In the model, a domain is divided into several rectangular subdomains in x and y directions. Each computing core stores and processes only information for elements located in a single subdomain. The cores communicate every time step with only a few cores that correspond to adjacent subdomains for synchronizing the information of elements located near boundaries of subdomains. If elements cross a subdomain boundary, they are transferred from one core to the other. At a certain interval, the size of all subdomains is adjusted to make loads on cores as even as possible. In this study, 2-64 cores are typically used for each simulation.

**Measurement of frequency-dependent elastic moduli**

We evaluated frequency-dependent elastic storage (*E*') and loss moduli (*E*"), by measuring stress in response to a small sinusoidal strain (10%) applied to the +x boundary of the rectangle domain with the –x boundary fixed. They were calculated in a similar way to that described in (1).

**Interactions between actin filaments and boundaries**

Boundaries without a periodic boundary condition (PBC) exert repulsive forces to actin filaments that are not clamped for volume-exclusion effects. Under reference conditions, we generated a network with $<L_f>$ = 0.9 μm in a rectangular domain (5 x 5 x 1 μm) with PBC only in x and y directions, and then deactivated PBC in x direction for measurement of creep. During simulations, few filaments had a length greater than 5 μm, and $<L_f>$ remained at ~0.9 μm due to the controlled nucleation rate and symmetric polymerization/depolymerization rates. Therefore, severing filaments for avoiding size-effects was unnecessary at mid of simulations.

TABLE S1 List of model parameters.

| Variable | Symbol | Value |
|---|---|---|
| Length of cylindrical actin segments | $r_{0,A}$ | $1.4\times10^{-7}$ [m] |
| Diameter of cylindrical actin segments | $r_{c,A}$ | $7.0\times10^{-9}$ [m] (1) |
| Bending angle of actin | $\theta_{0,A}$ | 0 [rad] (1) |
| Extensional stiffness of actin | $\kappa_{s,A}$ | $4.2\times10^{-3}$ [N/m] |
| Bending stiffness of actin | $\kappa_{b,A}$ | $2.64\times10^{-19}$ [N m] (2) |
| Length of a single arm of ACP | $r_{0,ACP}$ | $3.5\times10^{-8}$ [m] (3) |
| Diameter of a single arm of ACP | $r_{c,ACP}$ | $1.0\times10^{-8}$ [m] (3) |
| Bending angle 1 of ACP | $\theta_{0,ACP1}$ | 0 [rad] (1) |
| Bending angle 2 of ACP | $\theta_{0,ACP2}$ | $\pi$ / 2 [rad] (1) |
| Extensional stiffness of ACP | $\kappa_{s,ACP}$ | $4.23\times10^{-4}$ [N/m] |
| Bending stiffness 1 of ACP | $\kappa_{b,ACP1}$ | $1.04\times10^{-18}$ [N m] (1) |
| Bending stiffness 2 of ACP | $\kappa_{b,ACP2}$ | $4.142\times10^{-18}$ [N m] (1) |
| Strength of repulsive force | $\kappa_r$ | $4.23\times10^{-4}$ [N/m] |
| Concentration of actin | $C_A$ | 20-100 [μM] |
| Ratio of $C_{ACP}$ to $C_A$ | $R$ | 0.001-0.04 |
| Average length of actin filaments | $<L_f>$ | 0.6-6.5 [μm] |
| Time step | $\Delta t$ | $2.3\times10^{-6}$ [s] |
| Viscosity of medium | $\eta_m$ | $8.6\times10^{-2}$ [kg/m s] |

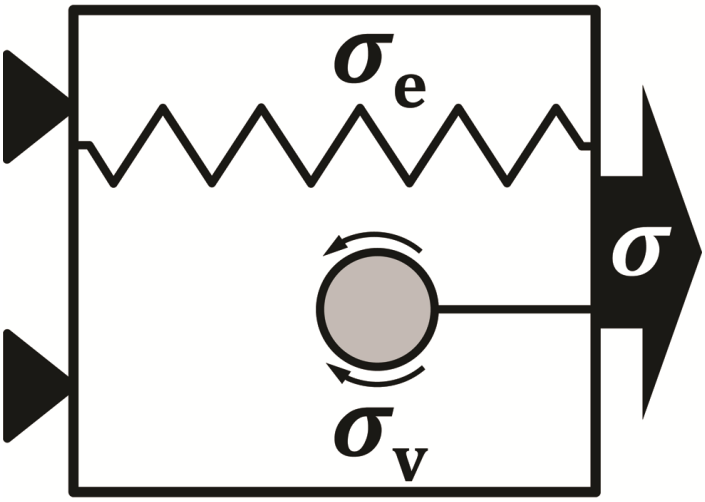


FIGURE S1 Decomposition of supporting stress into elastic and viscous components. The elastic stress $\sigma_e$ is sustained by elastic structures that percolate between the left and right boundaries. The viscous stress $\sigma_v$ originates from viscous drag forces on the portion of the network that is connected to the right boundary.

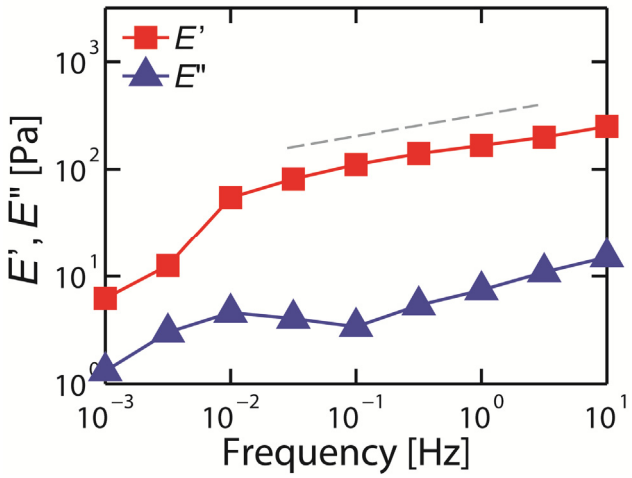


FIGURE S2 Frequency-dependent elastic storage ($E$', red squares) and loss moduli ($E$", blue triangles) with $n$ = 0.1 at 0.001-10 Hz. $E$' measures stored energy, indicating the elastic portion while $E$" measures dissipated energy, indicating the viscous portion. $E$' is much greater than $E$" at all frequencies, indicating that the network with $n$ = 0.1 exhibits a very elastic response and supporting the idea that the creep response is dominated by dissipation of elastic stress. Both $E$' and $E$" show a characteristic fall off at $f \leq 0.01$ Hz. A dashed line indicates $\sim f^{0.2}$.

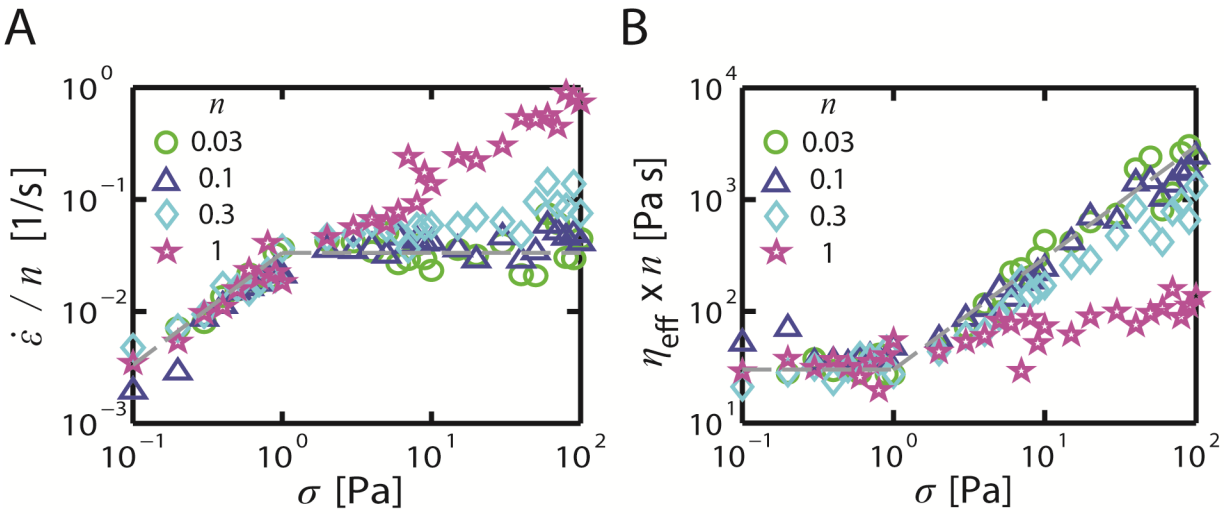


FIGURE S3 Transition between stress-dependent (linear) and stress-independent (non-linear) regimes persists over a range of network turnover rates ($n$). ($A$) $\dot{\varepsilon}/n$ vs $\sigma$ and ($B$) $\eta_{eff} \times n$ vs $\sigma$ for $n$ = 0.03 (green circles), 0.1 (blue triangles), 0.3 (cyan diamonds), and 1 (magenta stars). For $n \leq$ 0.3, all curves collapse onto a single master curve. For higher $n$, viscous resistance $\sigma_v$ becomes more dominant (see Fig. 2$B$), and the dependence of $\eta_{eff}$ on $\sigma$ is reduced. Dashed lines in ($A$-$B$) represent either $\sim\sigma^1$ or $\sim\sigma^0$.

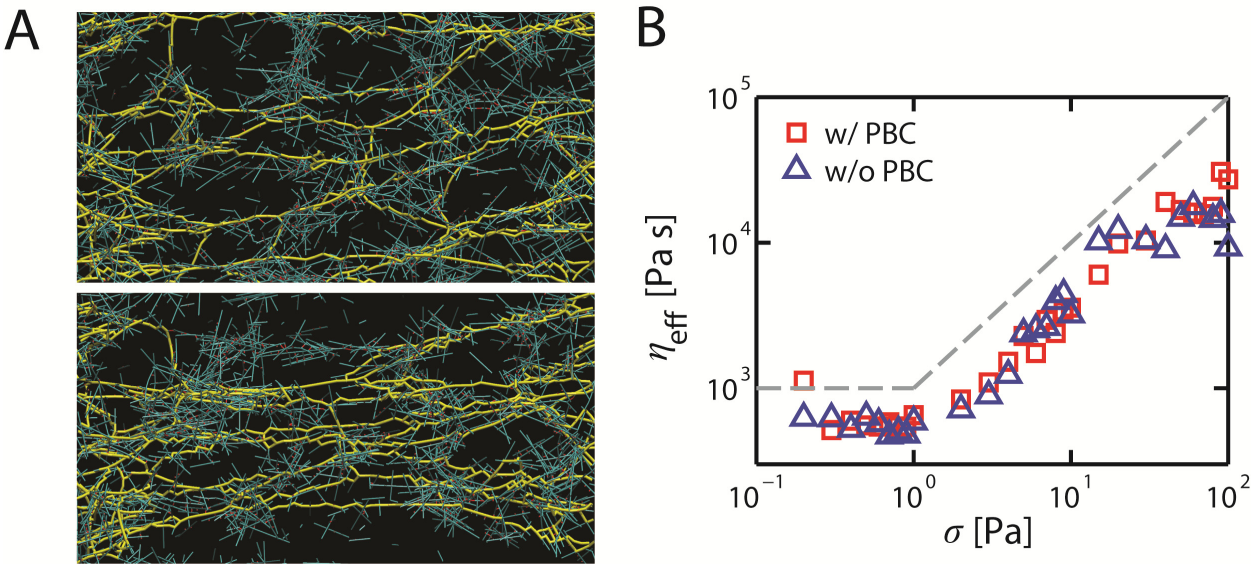


FIGURE S4 Effects of periodic boundary conditions (PBC) on simulated creep. ($A$) Snapshots of a network with $n$ = 0.1 and $\sigma$ = 100 Pa at $\varepsilon$ = 0.9 during the creep response with (top) or without PBC (bottom) in the y direction. Network-spanning (or percolating) pathways are shown by yellow in the network comprising actins (cyan) and ACPs (red). ($B$) $\eta_{eff}$ vs $\sigma$ with (blue triangles) or without PBC (red squares). Dashed lines represent either $\sim\sigma^1$ or $\sim\sigma^0$.

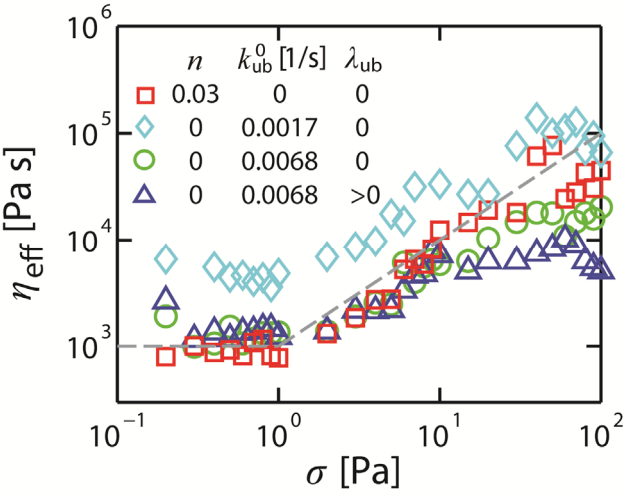


FIGURE S5 Comparison of $\eta_{eff}$ vs $\sigma$ for different modes of cross-link detachment: actin deploymerization (red squares); force-independent ACP unbinding (cyan diamonds and green circles); force-dependent ACP unbinding (blue triangles). Relevant parameter values are shown in the legend. Biphasic dependence on $\sigma$ emerges regardless of detachment modes. Actin depolymerization with $n$ = 0.03 (red squares) yields an effective ACP unbinding rate of 0.0017, but shows four-fold lower effective viscosity than pure unbinding at $k^0_{ub}$ = 0.0017/sec (cyan diamonds) due to differences in rebinding rates (not shown). For $k^0_{ub}$ = 0.0068 (green circles), $\eta_{eff}$ becomes similar to the case with $n$ = 0.03. Adding force dependence to the basal unbinding rate of $k^0_{ub}$ = 0.0068 (blue triangles) leads to a decrease of $\eta_{eff}$ for $\sigma$ > ~10 Pa. Dashed lines indicate either ~$\sigma^1$ or ~$\sigma^0$.

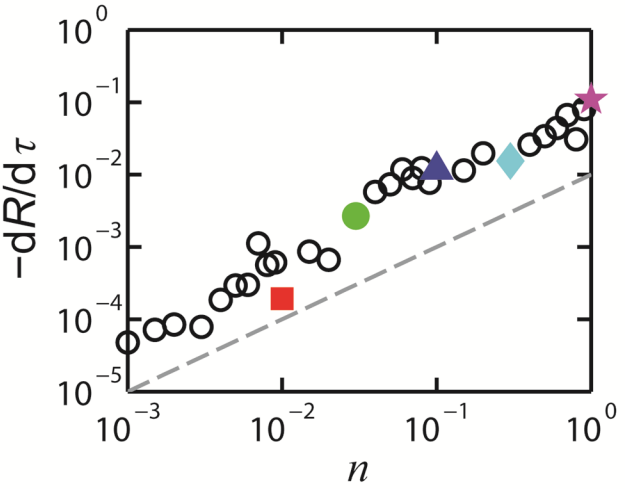


FIGURE S6 The slope of the autocorrelation function of tensions ($-dR/d\tau$) vs $n$ for $\sigma$ = 10 Pa. Tensions on individual actin filaments decay at a rate proportional to network turnover ($n$). Colored symbols correspond to the colored traces in Fig. 2*A*. The dashed line indicates ~$n^1$.

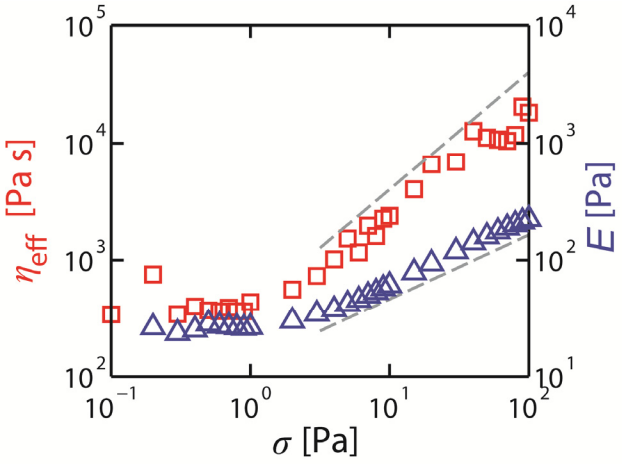


FIGURE S7 Comparison of $\eta_{eff}$ vs $\sigma$ at $n = 0.1$ (red squares) with $E$ vs $\sigma$ (blue triangles). $E$ is measured as $\sigma$ divided by $\varepsilon$ at a steady state at $n = 0$. Both $\eta_{eff}$ and $E$ are independent of $\sigma$ at $\sigma < 1$ Pa but show proportionality to $\sigma$ at $\sigma > \sim 1$ Pa. Dashed lines represent either $\sim\sigma^1$ or $\sim\sigma^{0.55}$.

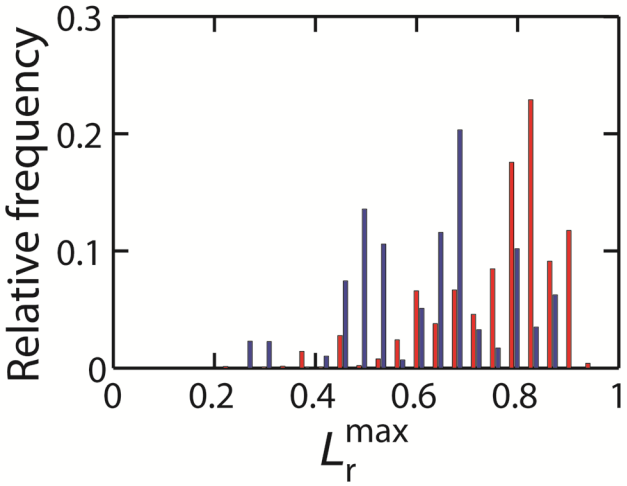


FIGURE S8 Distribution of maximum relative extension ( $L_r^{max}$ ) during the lifetime of individual sub-segments. The distribution is measured for all sub-segments at $n = 0.1$ in response to either low ($\sigma = 0.2$ Pa, blue) or high ($\sigma = 10$ Pa, red) stress.

MOVIE S1 Deformation of networks during the creep with $n$ = 0.1. The top row shows the network-spanning (or percolating) pathways (yellow) between two boundaries whose length is not greater than 2×[instantaneous domain width in x-direction]. Cyan stands for actin filaments, and red represents ACPs. The bottom row in the movie shows the tension level by color scaling. Compressive forces are changed to zero represented by blue, and tensions greater than 10 pN are shown by red. White shows intermediate levels of tensions.

**SUPPORTING REFERENCES**


1. Kim, T., W. Hwang, H. Lee, and R. D. Kamm. 2009. Computational analysis of viscoelastic properties of crosslinked actin networks. PLoS Comput Biol 5:e1000439.
2. Isambert, H., P. Venier, A. C. Maggs, A. Fattoum, R. Kassab, D. Pantaloni, and M. F. Carlier. 1995. Flexibility of actin-filaments derived from thermal fluctuations - effect of bound nucleotide, phalloidin, and muscle regulatory proteins. J Biol Chem 270:11437-11444.
3. Meyer, R. K. and U. Aebi. 1990. Bundling of actin-filaments by alpha-actinin depends on its molecular length. J Cell Biol 110:2013-2024.